Intermodulation Nulling in HEMT Common Source Amplifiers

Anthony E. Parker, *Senior Member, IEEE,* and Guoli Qu

***Abstract*—A new model of the second- and third-order intermodulation products from HEMT and MESFET small-signal amplifiers, resulting from nonlinear drain-source current has been proposed in our previous publications. Based on this model, intermodulation nulling conditions in terms of the Taylor series coefficients, hence in terms of bias, have been investigated. This paper now examines the load dependence of the second- and third-order intermodulation products in HEMT small-signal common source amplifiers. Intermodulation nulling conditions are proposed and validated. This is useful in designing a high performance amplifier by calculation of optimum load for minimum distortion and studying distortion generation as a function of circuit topology.**

***Index Terms*—HEMTs, intermodulation distortion, MODFETs, nonlinear distortion, volterra series.**

I. Introduction

In order to analyze the dependence of intermodulation distortion on intrinsic and extrinsic elements and to design low distortion amplifiers, we proposed a model [1] of the second- and third-order intermodulation products resulting from weakly nonlinear drain-source current for small-signal HEMT and MESFET amplifiers, based on the Volterra analysis [2]. This model gives quantitative expressions for intermodulation in terms of load and the coefficients of a two-dimensional (2–D) Taylor series expansion of nonlinear drain-source current. The contribution of the second-order terms in the 2–D Taylor series expansion to the third-order intermodulation as well as the contribution of cross-terms to overall intermodulation products are included in the model. The inclusion of these terms is proven to be significant, especially when the model is used to predict regions of intermodulation reduction that occurs at certain biases and loads [1], [3]. It should be noted that this analysis is applicable to weakly nonlinear applications with low-level signals. The contribution of the higher-order coefficients to the second and/or third order IM distortion is therefore ignored. Based on the model proposed in [1], intermodulation nulling conditions in terms of the Taylor series coefficients, hence in terms of bias, were reported in [3]. In this paper the load dependence of IM products is examined and intermodulation nulling conditions are proposed and validated.

Manuscript received July 26, 2000; revised December 6, 2000.

The authors are with Electronics Department, Macquarie University, Sydney 2109, Australia (e-mail: tonyp@ieee.org; tonyp@elec.mq.edu.au).

Publisher Item Identifier S 1531-1309(01)03214-7.

II. Load Dependence and Intermodulation Cancellation

If the input $v_{\rm in}$ is assumed to be a low-level two-tone excitation of the form

$$v_{\rm in} = V_s(\cos\omega_1 t + \cos\omega_2 t). \tag{1}$$

Then the output drain current is given by

$$\begin{aligned} i_{ds} = {} & g_m v_{gs} + G_{ds} v_{ds} \\ & + \tfrac{1}{2}\left(g'_m v_{gs}^2 + G'_{ds} v_{ds}^2 + 2m_{11} v_{gs} v_{ds}\right) \\ & + \tfrac{1}{6}\left(g''_m v_{gs}^3 + G''_{ds} v_{ds}^3 + 3m_{12} v_{gs} v_{ds}^2 + 3m_{21} v_{gs}^2 v_{ds}\right) \end{aligned} \tag{2}$$

where the coefficients g_m, g'_m and g''_m respectively are transconductance and its derivatives with respect to v_{gs}; the coefficients G_{ds}, G'_{ds} and G''_{ds} respectively are the drain-source conductance and its derivatives with respect to v_{ds}; and the coefficients

$$\begin{aligned} m_{11} &= \partial g_m/\partial v_{ds} = \partial G_{ds}/\partial v_{gs}, \\ m12 &= \partial^2 g_m/\partial v_{ds}^2 = \partial G'_{ds}/\partial v_{gs} \end{aligned}$$

and

$$m_{21} = \partial g'_m/\partial v_{ds} = \partial^2 G_{ds}/\partial v_{gs}^2$$

are cross terms.

With this model, the linear (P_{lin}), second- ($P_{\rm IM2}$) and third-order ($P_{\rm IM3}$) IM output powers into a load R_L can be expressed, in dBm, as [1]

$$P_{lin} = 10\log\left[\tfrac{1}{2}\left(g_m + G_{ds}A_v\right)^2 V_s^2 R_L\right] + 30 \tag{3}$$

$$P_{\rm IM2} = 10\log\left[\frac{R_e^2}{8R_L}\left(g'_m + G'_{ds}A_v^2 + 2m_{11}A_v\right)^2 V_s^4\right] + 30 \tag{4}$$

$$\begin{aligned} P_{\rm IM3} = 10\log\Bigg\{\frac{R_e^2}{128R_L}\Big[\left(g''_m + G''_{ds}A_v^3 + 3m_{12}A_v^2 + 3m_{21}A_v\right) \\ - 3R_e\left(g'_m + G'_{ds}A_v^2 + 2m_{11}A_v\right) \\ \cdot\left(G'_{ds}A_v + m_{11}\right)\Big]^2 V_s^6\Bigg\} + 30. \end{aligned} \tag{5}$$

By substituting the amplifier voltage gain, $A_v = (-g_m R_L)/(1 + G_{ds}R_L) = -g_m R_e$, into the above equations, they can be expressed as

$$P_{lin} = 10\log\left(\frac{1}{2}\,g_m^2 V_s^2\right) + 10\log\left[\frac{R_L}{(G_{ds}R_L + 1)^2}\right] + 30 \tag{6}$$

$$P_{\mathrm{IM2}} = 10\log\left[\frac{R_e^2}{8R_L}\left(g_m' + G_{ds}' g_m^2 R_e^2 - 2m_{11} g_m R_e\right)^2 V_s^4\right] + 30 \tag{7}$$

$$P_{\mathrm{IM3}} = 10\log\left\{\frac{9}{32R_L}\left[\frac{R_e}{6}\left(g_m'' - G_{ds}'' g_m^3 R_e^3 + 3m_{12} g_m^2 R_e^2 - 3m_{21} g_m R_e\right) - \frac{R_e^2}{2} \cdot \left(g_m' + G_{ds}' g_m^2 R_e^2 - 2m_{11} g_m R_e\right) \cdot \left(m_{11} - G_{ds}' g_m R_e\right)\right]^2 V_s^6\right\} + 30 \tag{8}$$

where $R_e = R_L/(1 + G_{ds}R_L)$ is the net load resistance, being R_L in parallel with the HEMT output conductance G_{ds}.

In the saturation region ($V_{ds} \gg 1$ V), it can be assumed that G_{ds}' and G_{ds}'' are zero [4]. The cross terms are normally more important than output conductance. However, they can also be ignored [5]. With these assumption, Equations (7) and (8) are reduced to

$$P_{\mathrm{IM2}} = 10\log\left(\frac{1}{8} {g_m'}^2 V_s^4\right) + 10\log\left[\frac{R_L}{(G_{ds}R_L + 1)^2}\right] + 30 \tag{9}$$

$$P_{\mathrm{IM3}} = 10\log\left(\frac{1}{128} {g_m''}^2 V_s^6\right) + 10\log\left[\frac{R_L}{(G_{ds}R_L + 1)^2}\right] + 30. \tag{10}$$

As seen in (6), (9), and (10) P_{lin}, P_{IM2}, and P_{IM3} have the same R_L dependence, which follows $\log[R_L/(G_{ds}R_L + 1)^2]$. If R_L is small, i.e., when $G_{ds}R_L \ll 1$, then P_{lin} P_{IM2} and P_{IM3} increase logarithmically with the increasing of R_L. If R_L is large, the G_{ds} cannot be ignored and P_{lin}, P_{IM2} and P_{IM3} are proportional to $\log[R_L/(G_{ds}R_L + 1)^2]$.

From (7), IM2 cancellation occurs when

$$G_{ds}' g_m^2 R_e^2 - 2m_{11} g_m R_e + g_m' = 0. \tag{11}$$

That is, IM2 cancellation occurs when R_e, hence $R_L = R_e/(1 - G_{ds}R_e)$, satisfies the above equation. For clarity, (11) can be rewritten as

$$R_L = \frac{2m_{11}g_m + \sqrt{4m_{11}^2 g_m^2 - 4G_{ds}' g_m^2 g_m'}}{2G_{ds}' g_m^2 - G_{ds}\left(2m_{11}g_m + \sqrt{4m_{11}^2 g_m^2 - 4G_{ds}' g_m^2 g_m'}\right)}. \tag{12}$$

Note that the dependence of R_L for IM2 cancellation on the coefficients G_{ds}' and m_{11} should not be ignored.

Similarly, IM3 cancellation occurs when R_e, and hence R_L, satisfies the following equation:

$$g_m'' - G_{ds}'' g_m^3 R_e^3 + 3m_{12} g_m^2 R_e^2 - 3m_{21} g_m R_e - 3R_e\left(g_m' + G_{ds}' g_m^2 R_e^2 - 2m_{11} g_m R_e\right) \cdot \left(m_{11} - G_{ds}' g_m R_e\right) = 0. \tag{13}$$

The cross terms and the coefficients G_{ds}', G_{ds}'' should not be ignored when determining R_L for IM3 cancellation.

Fig. 1 shows the dependence on R_L of IM products for a ATF-36 163 HEMT common-source amplifier simulated with SPICE. In the simulation, the model is the one proposed in [6] with the model parameters used in [6, Figs. 1–3], which has been

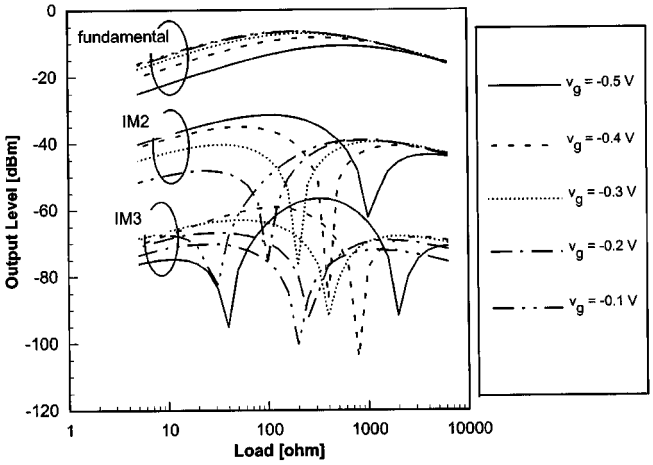

Fig. 1. SPICE simulated IM products as a function of R_L for an ATF-36 163 common source amplifier biased at $V_{ds} = 2$ V with -23 dBm input tones.

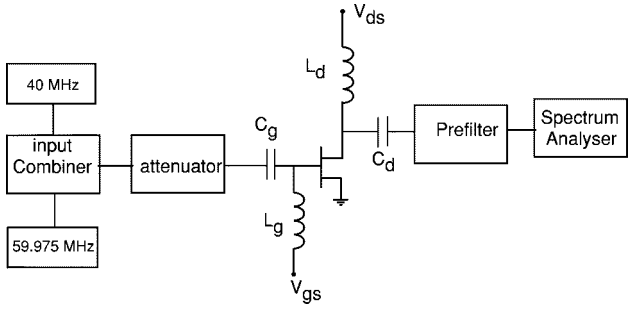

Fig. 2. Intermodulation measurement setup.

verified to predict IM products accurately over a wide range of bias. Note that the results in Fig. 1 are really the intermodulation behavior of the nonlinear equations used in this SPICE model. However, they do provide a good representation of the intermodulation behavior of the fitted device and demonstrate the nulling dependencies. That is, Fig. 1 shows that at low values of R_L, the power levels P_{lin}, P_{IM2} and P_{IM3} increase at the expected logarithmic rate with R_L with IM cancellation occurring at certain load values. Note that P_{lin} drops for high values of R_L because G_{ds} is significant and the term $\log[R_L/(G_{ds}R_L + 1)^2]$ in (6) drops with increasing R_L. The larger the value of R_L, the more significant is the effect of G_{ds}.

A Taylor series description fitted to each bias point gives more accurate low-signal results than a large-signal SPICE model. To show the R_L dependency and IM cancellation effects, the IM calculations from Taylor series coefficients with (7) and (8) were performed and compared with measurements. The ATF-36 077 common-source amplifier biased at $V_{gs} = -0.5$ V, $V_{gs} = -0.3$ V and $V_{gs} = -0.1$ V was used as the test device. Measurements were performed with TDFD technique [5] with the device under common-source amplifier configuration. Measurement setup is shown in Fig. 2. In the calculation, the nine Taylor series coefficients are extracted from four groups of measured IM products with different loads [7]. This group of coefficients can well predict IM products at a wide range of bias as shown in Fig. 3. The calculation with (7) and (8) agrees well with measurements as shown in Fig. 4.

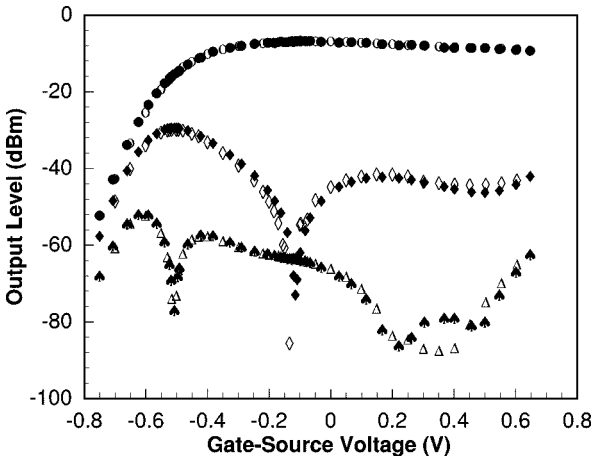

Fig. 3. Fundamental (upper lines), second-(middle lines) and third-order (bottom lines) IM output levels of a ATF-36 077 HEMT common-source amplifier biased at $V_{ds} = 2$ V with input tones at -23 dBm and a 50 Ω load. Solid symbols: measurement; open symbols: calculations with the model using the coefficients extracted from measured IM data of four other loads.

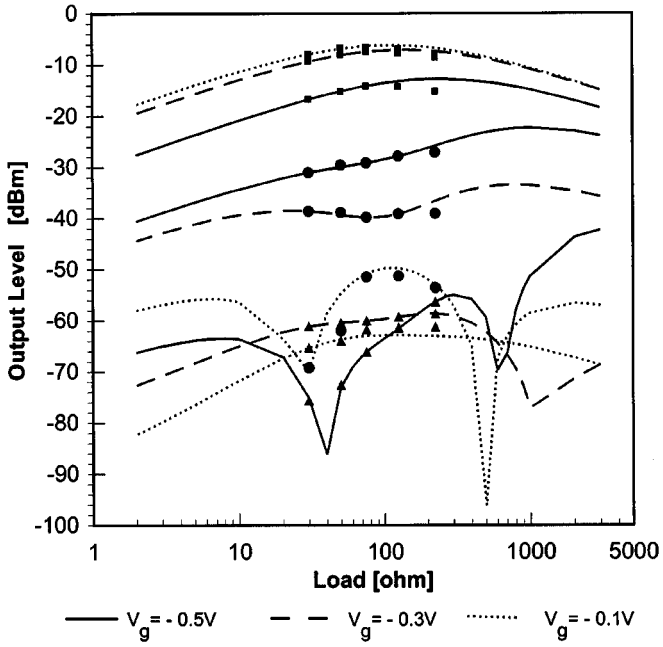

Fig. 4. Calculated with (4)–(6) (lines) and measured fundamental (■), second-(•) and third-order (▲) intermodulation products of an ATF-36 077 common source amplifier biased at $V_{ds} = 2$ V with -23 dBm input tones as a function of R_L.

Both Figs. 1 and 4 clearly demonstrate the cancellation effects, which are predicted by (11) and (13).

For cancellation of IM2 the load R_L is given by (12), which is a rearrangement of (11). This is a complicated function of bias and load and show that cancellation may not always be achievable at specific bias conditions with resistive loads. The cancellation of IM2 shown in Fig. 4 only occurs for $V_g = -0.1$ V and not at the other gate potentials shown. The lack of cancellation occurs when R_L from (12) is complex. For cancellation of IM3, R_L can be determined by a similar rearrangement of (13) and exhibits a similar complexity. The importance of these equations is that they allow prediction and assessment of this aspect of device nonlinearity.

III. Conclusion

The dependence of intermodulation distortion on load R_L is analyzed when the HEMT operates in the saturation region. When R_L is small, the fundamental, second- and third-order IM levels increase approximately at a logarithmic rate with increasing R_L. For high values of R_L, IM2 and IM3 cancellations occur when R_L (hence R_L) satisfies the conditions in (11) and (13) respectively. It should be noted that IM cancellation effects cannot be predicted without considering the contribution of the second-order terms in Taylor series to the third-order intermodulation as well as the contribution of cross-terms to overall intermodulation products. This work confirms the significance of these contributions to the model, which was also discussed in [3], [5]. In small-signal applications these are more significant than the contribution of the higher-order coefficients to the second and/or third order IM distortion, which can be ignored. The IM cancellation conditions (11) and (13) are validated by comparing measurements and calculations.

As long as the Taylor series coefficients are extracted correctly, the load required for minimum IM distortion can be predicted by using IM cancellation conditions (11) and (13). In other words, once the device is characterized in terms of its Taylor series coefficients, the load can be selected to maximize IM performance. Although it is not practical to make the circuit to operate exactly in the IM nulling condition due to the sensitivity of nulling phenomena, these results provide guidelines for circuit designers to select the bias and load to position operation in regions of reduced distortion. Moreover, the model is useful for exploring the generation of distortion in various applications.

References

[1] G. Qu and A. E. Parker, "Modeling intermodulation distortion in MESFET's and HEMT's," in *Proc. 14th Australian Microelectronics Conf.*, Sept. 29-Oct. 1, 1997, pp. 70–75.

[2] S. A. Maas, *Nonlinear Microwave Circuits*. Boston, MA: Artech House, 1988.

[3] G. Qu and A. E. Parker, "Intermodulation cancellation in HEMT's," in *Proc. 1998 Int. Conf. Microwave and Millimeter Wave Technology*, Aug. 18–20, 1998, pp. 84–87.

[4] ——, "Analysis of intermodulation nulling in HEMTs," in *Proc. Conf. Optoelectronic and Microelectronic Materials and Devices*, Canberra, Australia, Dec. 1996, pp. 227–230.

[5] G. Qu, "Characterizing intermodulation in high electron mobility transistors," Ph.D. dissertation, Macquarie Univ., Sydney, Australia, 1998.

[6] G. Qu and A. E. Parker, "Validation of a new high electron mobility transistor SPICE model," in *Proc. IEEE MTT-S Int. Microwave Symp.*, Baltimore, MD, June 7–12, 1998.

[7] ——, "New model extraction for predicting distortion in HEMT and MESFET circuits," *IEEE Microwave Guided Wave Lett.*, vol. 9, pp. 363–365, Sept. 1999.